

PSIM and MATLAB based Simulation of Photovoltaic Array with MPPT Algorithm for DC to DC Converter

Ajit Pratpa Singh¹, Prof. Upendra Singh Tomar², Prof. Mangesh Singh Tomar³

PG Student, Department of Electrical Engineering¹

Assistant Professor, Department of Electrical Engineering²

Assistant Professor, Department of Electronics Engineering³

Vikrant Institute of Technology & Management, Gwalior, India

Abstract: Solar energy is the most vital energy resource now a day since it is clean, pollution free, and inexhaustible. Semiconductor gave the crucial support due to its rapid growth in the power electronics techniques. In this paper, the maximum power point technique is used to increase the output efficiency of PV arrays. The output power of PV arrays changes with weather conditions, which means solar irradiation and atmospheric temperature. A perturbation and observation (P&O) method used to track the maximum power point of PV array voltage. To track the maximum voltage, we used boost converter and simulated the circuit on Matlab and PSIM.

Keywords: Modelling of PV arrays, boost converter, perturbation and observation method and simulation results.

I. INTRODUCTION

A photovoltaic framework changes over daylight into power. The essential gadget of a photovoltaic framework is the photovoltaic cell. Cells might be gathered to shape boards or modules. Boards can be assembled to shape vast photovoltaic clusters. The term cluster is normally utilized to depict a photovoltaic board (with a few cells associated in arrangement as well as parallel) or a gathering of boards. The term exhibit is utilized from now on which means any photovoltaic gadget made out of a few fundamental cells. The utilization of new proficient photovoltaic sun based cells (PVSCs) has developed as an option measure of renewable green power, vitality preservation and request side administration. The execution of a PV exhibit framework relies on upon the working conditions and additionally the sun oriented cell and cluster outline quality. The yield voltage, current and force of PV cluster change with elements of sunlight based light level, temperature and load current. Subsequently the impacts of these three amounts must be considered in the plan of PV clusters so that any adjustment in temperature and sun powered light levels, ought not unfavorably influence the PV exhibit yield to the heap/utility, which is either a power organization utility network or any remaining solitary electrical sort stack [1].

Perturbation and observation (P&O) can track the maximum power point (MPP) constantly, independent of the barometrical conditions, kind of PV board, and notwithstanding maturing, by handling genuine estimations of PV voltage and current. Since the cost of the required hardware for actualizing on-line MPPTs is higher, they are typically utilized for bigger PV exhibits. P&O technique is generally utilized as a part of PV frameworks due to its effortlessness and simple of execution. Be that as it may, it presents downsides, for example, moderate reaction speed, wavering around the MPP in unflinching state, and notwithstanding following in wrong route under quickly changing climatic conditions. To beat the above downsides of P&O strategy, gave that the calculation is completed at quick rates. They are typically in light of the correlation of normal estimations of "ipv" and "vpv" got from low-pass channels, which present deferrals, and on the control of the normal estimation of either "ipv" or "vpv" bringing about moderate velocities of response [2]. This proposes another execution of a P&O calculation that mitigates the principle downsides, ordinarily identified with the P&O method. Another perturbation and observation technique (IP&O) in view of fixed algorithm is proposed, which consequently changes the reference step size and hysteresis transfer speed for power examination. The IP&O builds the aggregate PV

yield control by 0.5% at an unsettled climate condition, in contrast with customary bother and perception strategy (P&O). The new iteration and perception (IP&O) has the following reaction will be affected. At the point when IP&O strategy has quickly changing air conditions then the skittish execution with motions around greatest power point (MPP). IP&O has high unwavering quality and it is extremely intricate. The new P&O technique is presented, in view of hysteresis band and auto-tuning annoyance step. There is exchange off between element reaction and relentless state because of the determination of "dv" [3-7].

II. PV GENERATOR

A photovoltaic PV generator is the entire gathering of solar cells, associations, defensive parts, underpins and so forth. In the present display, the emphasis is just on cell/module/ exhibit. Sun powered cells comprise of a p-n intersection manufactured in a thin wafer or layer of semiconductor (generally silicon) [8].

Modeling the Solar Cell

In this way, the most straightforward proportionate circuit of a sunlight based cell is a present source in parallel with a diode. The yield of the present source is specifically corresponding to the light falling on the phone (photocurrent I_{ph}). Amid dimness, the sun oriented cell is not a dynamic gadget. It fills in as a diode [9-16].

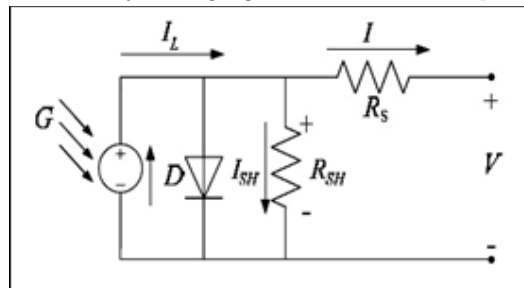


Fig. 1: Equivalent Circuit of PV Panel.

2.2 PV Cell Circuit

The working state of the solar cell depends primarily on the heap and solar isolation. They work in the open circuit mode and short circuit mode. Based on these attributes, the yield voltage, current and power can be calculated.

I_{ph} : Photodiode current, V_d : Diode voltage,

I_d : Diode current n-Diode factor (1 for ideal and >2 for real).

In an ideal cell $R_s=R_{sh}=0$, which is a relatively common assumption. In this paper, the equation of PV equivalent circuit is given below

$$I = I_L - I_0 \left(e^{\frac{e(V+IR\delta)}{mKT}} - 1 \right)$$

$$I_L = I_L(T_1) + K_0(T - T_1)$$

$$I_L(T_1) = I_{SC}(T_{1NOM}) \frac{G}{G_{NOM}}$$

$$K_0 = \frac{I_{SC}(T_2) - I_{SC}(T_1)}{(T_2)}$$

$$I_0 = I_0(T_1) * \left(\frac{T}{T_1} \right)^{\frac{n}{3}} e^{\frac{qV}{nk} \left(\frac{1}{T} - \frac{1}{T_1} \right)}$$

$$I_0(T_1) = \frac{I_{SC}(T_1)}{\left(e^{\frac{qV_{sc}(T_1)}{nkT_1}} - 1 \right)}$$

A series resistance R_s represents

$$R_s = -\frac{dV}{dI_{VOC}} - \frac{1}{X_V}$$

$$X_V = I_0(T_1) \frac{q}{nkT_2} e^{\frac{eV_{sc}(T_1)}{nkT_1}} - \frac{1}{X_V}$$

The shunt resistance R_{sh} is neglected. A single shunt diode was used with the diode quality factor set to achieve the best curve match. This model is a simplified version of the two diode model presented by Gow and Manning. The circuit diagram for the solar cell is shown in Figure 2.

$$P_{max} = I_{ph} \left\{ V_{oc} - \frac{nkT}{q} \ln(1 + qV_{mppt}/nkT) - V_{oc} / (qV_{mppt}/nkT) + nkT/2 \right\} (1/V_{mppt}) \ln(1 + qV_{mppt}/nkT)$$

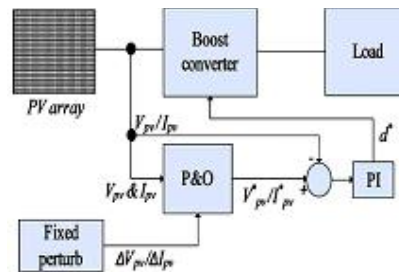


Fig. 2: Fixed Perturb with Perturbation and Observation.

III. P&O METHOD

In this strategy, a constant perturb value is used to create a reference motion for the external control loop. The perturb flag is either the exhibit reference voltage or current. The settled irritate step is resolved by the framework. Accordingly, the arrangement given by this technique is not nonspecific and framework subordinate. For little bother steps, the following is moderate yet the power/voltage motions are insignificant. On account of vast irritate step, quicker following is accomplished with expanded motions. Consequently, P&O systems with settled bother endure an inborn tracking oscillations irradiance changes gradually, yet the P&O strategy neglects to track the MPP when irradiance changes all of a sudden by having moderate element response [19].

Mode 1 Operation of the Boost Converter

At the point when the switch is off, the inductor gets charged through the battery and energy is stored. In this state, the inductor current ascends (exponentially), yet for effortlessness we expect that the charging and the discharging of the inductor are straight. The diode hinders the flow of current, thus the heap current stays steady which is being provided because of the discharging of the capacitor [20] (Figure 4).

Mode 2 Operation of the Boost Converter

In mode 2, the switch is open, thus the diode turns out to be short circuited and the energy that is stored in the inductor gets released through inverse polarities, which charge the capacitor (Figure 5). The heap current stays consistent all through the operation. The waveforms for a boost converter are illustrated through Figures 6 and 8.

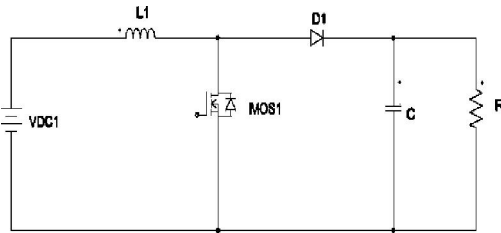


Fig. 3: Circuit Diagram of a Boost Converter.

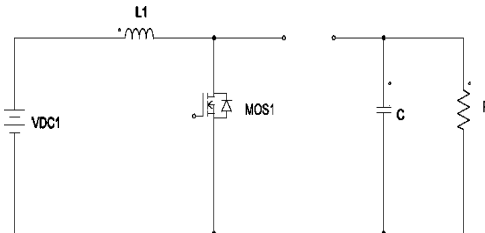


Fig. 4: Mode 1 Operation of Boost Converter.

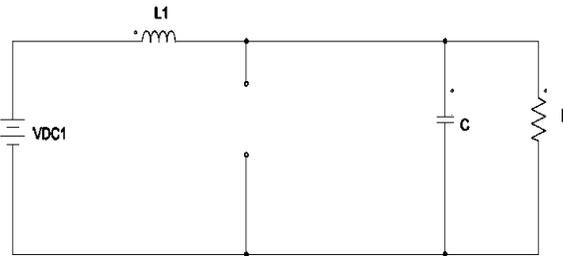


Fig. 5: Mode 2 Operation of Boost Converter.

IV. UNMASKED BLOCK DIAGRAM OF THE MODELED SOLAR PV PANEL AND THEIR WAVEFORM

The simulation is done for a cell surface temperature of 28°C, 60 solar cells in arrangement and four columns of sun based cells in parallel. The light is taken to shift, to reflect genuine conditions and successfully demonstrate the utilization of a MPPT calculation in field runs (Figure 9). It differs from 60 W to 85 W for each cm², which is near the day estimations of sun based radiation got on the world's surface. The recreation is kept running for an aggregate of 0.18 sec, with the illumination taking up another esteem like clockwork and remaining consistent for the resulting 0.05 sec [21–23].

V. PERTURB AND OBSERVE ALGORITHM

The perturb and observe algorithm is explained through Figure 7.

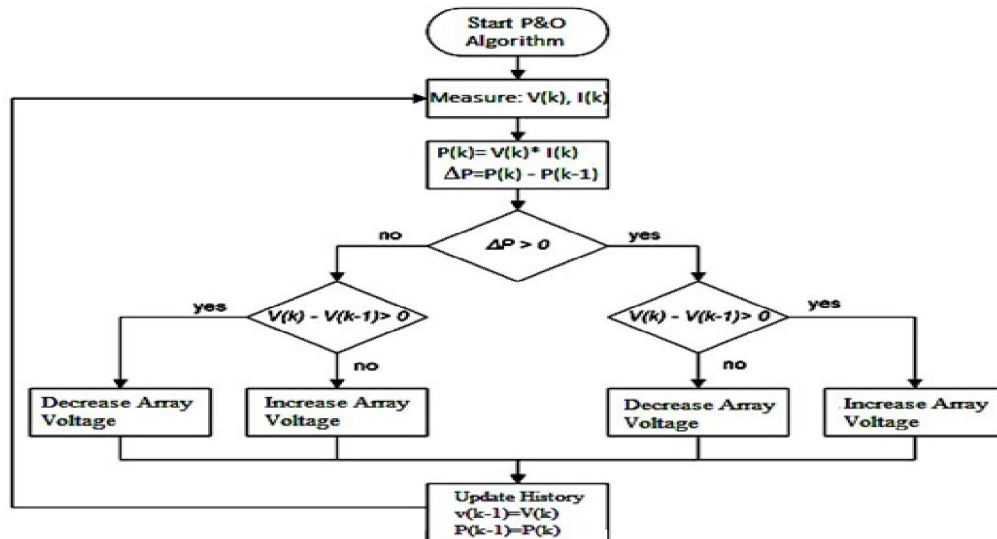


Fig. 7: Flow Chart Perturb and Observe Algorithm

VI. RESULT

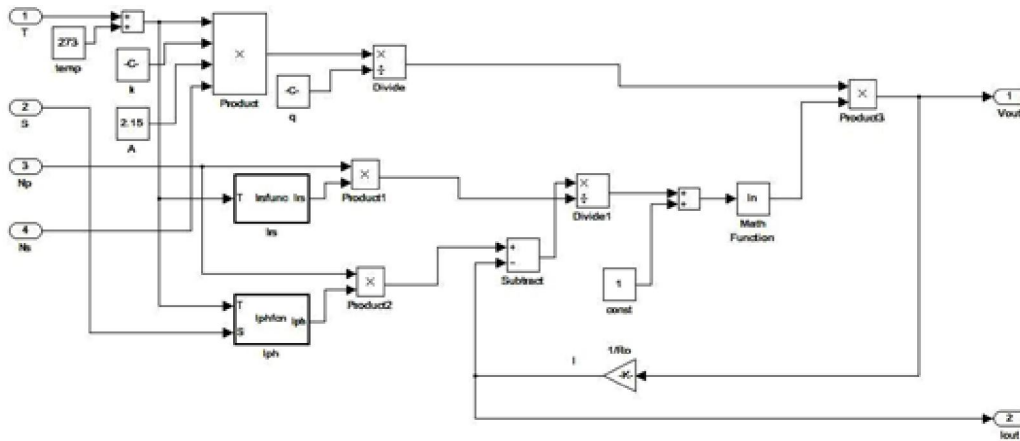


Fig. 8: Waveform of Boost Converter.

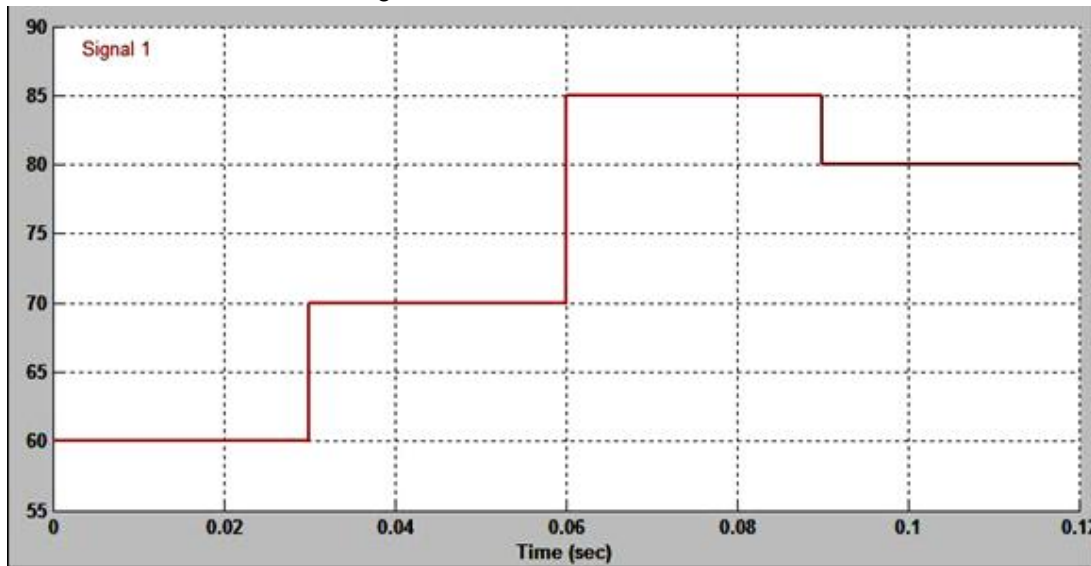


Fig. 9: Waveform of Boost Converter

Table 1: Different Parameters of the Standalone PV System

Parameter	Value taken for Simulation
Solar module temperature (T)	28°C
No. of solar cells in series (Ns)	60
No. of rows of solar cells in parallel (Np)	4
Resistance of load (R)	300
Capacitance of boost converter (C)	0.611 μF
Inductance of boost converter (L)	0.763 mH
Switching frequency of PWM	100 KHz
Proportional gain of PI controller (Kp)	0.006
Integral gain of PI controller (Ki)	7

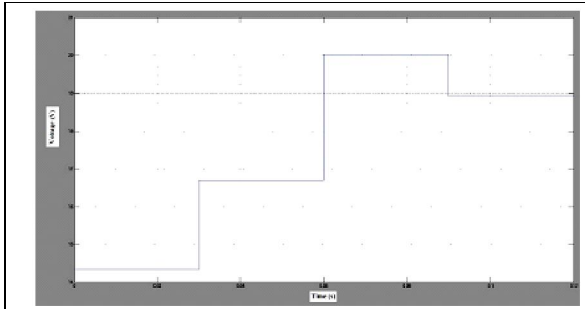


Fig. 10: Plot of Output Voltage of PV Panel versus Time without MPPT

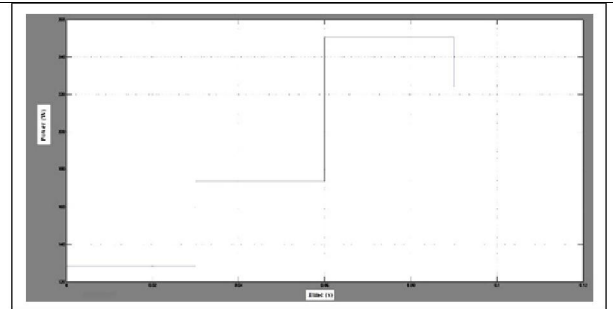


Fig. 11: Plot of Power Output of PV Panel versus Time without MPPT

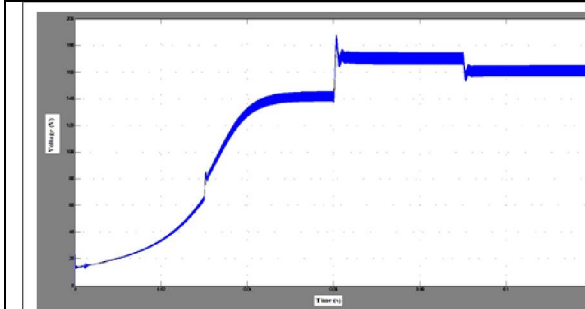


Fig. 12: Plot of Output Voltage at Load Side versus Time without MPPT

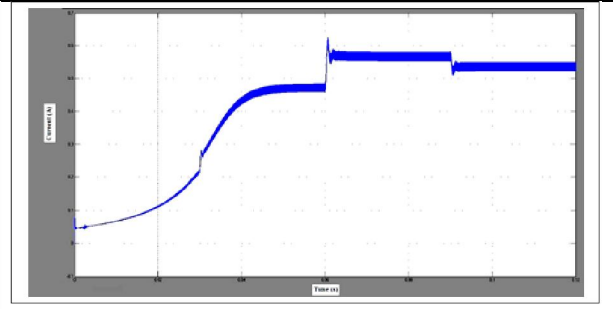


Fig. 13: Plot of Output Current at Load Side versus Time without MPPT

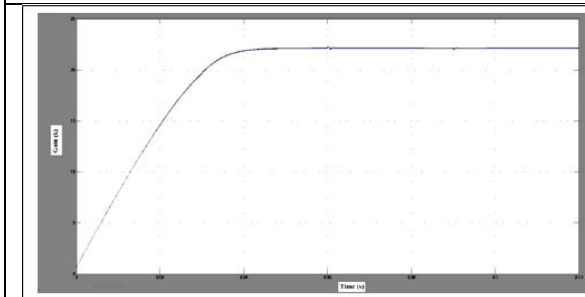


Fig. 14: Plot of PI Control Gain versus Time with MPPT

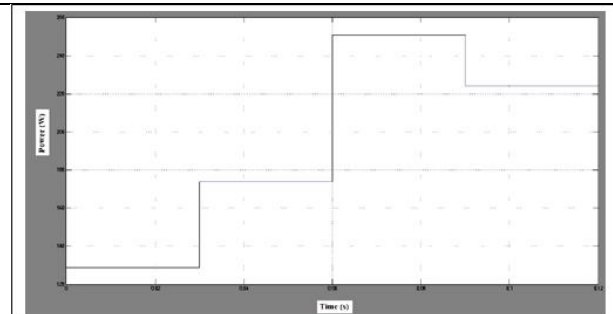


Fig. 15: Plot of Power Output of PV Panel versus Time with MPPT

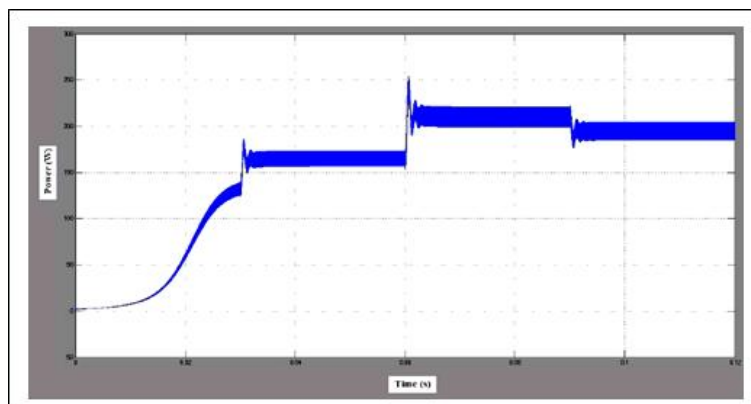


Fig. 16: Plot of Power Obtained at Load Side versus Time with MPPT

VII. CONCLUSION

The reenactment was then kept running with the switch on MPPT mode. This incorporated the MPPT hinder in the circuit and the PI controller was sustained, the V_{ref} as computed by the P&O calculation. Under a similar irradiation conditions, the PV board kept on creating around 250 W control (Figures 10–15). For this situation, the power acquired at the heap side was observed to be around 215 W (Figure 16), subsequently enhancing the change in effectiveness of the photovoltaic framework in general (Table 1).

The loss of force from the accessible 250 W produced by the PV board can be clarified by exchanging misfortunes in the high recurrence PWM exchanging circuit and the inductive and capacitive misfortunes in the boost converter circuit.

REFERENCES

- [1]. Femia N, Petrone G, Spagnuolo G. A Technique for Improving P&O MPPT Performances of Double-Stage Grid- Connected Photovoltaic Systems. *IEEE Trans Ind Electron.* Nov 2009; 56(11): 4473–4482p.
- [2]. Yuvarajan S, Shoeb J. A Fast and Accurate Maximum Power Point Tracker for PV Systems. *Applied Power Electronics Conference and Exposition, APEC 2008.* 167–172p. 2970.
- [3]. Hussein KH, Muta I, Hoshino T, et al. Maximum Photovoltaic Power Tacking: An Algorithm for Rapidly Changing Atmospheric Conditions. *Proc IEE, Generation, Transmission, Distribution.* 1 Jan 1995; 142.1\10: 59–61p.
- [4]. Buresch M. *Photovoltaic Energy Systems Design and Installation.* New York: McGraw-Hill; 1983.
- [5]. Savita Nema, Nema RK, Gayatri Agnihotri. *Matlab Simulink Based Study of Photovoltaic Cells Array and their Experimental Verification.* *IJEE.* 2010; 1(3): 487–500p.
- [6]. Ashish Kumar Singhal, Rakesh Narvey. *PSIM and Matlab based Simulation of PV Array for Enhance the Performance by using MPPT Algorithm.* *IJEE.* 2011; 4(5): 511–520p. ISSN 0974-2158.
- [7]. J. M. Guerrero, L. G. de Vicuna, J. Matas, M. Castilla, and J. Miret, “A wireless controller to enhance dynamic performance of parallel inverters in distributed generation systems,” *IEEE Trans. Power Electron.*, vol. 19, no. 5, pp. 1205–1213, Sep. 2004.
- [8]. J. H. R. Enslin and P. J. M. Heskes, “Harmonic interaction between a large number of distributed power inverters and the distribution network,” *IEEE Trans. Power Electron.*, vol. 19, no. 6, pp. 1586–1593, Nov. 2004.
- [9]. U. Borup, F. Blaabjerg, and P. N. Enjeti, “Sharing of nonlinear load in parallel- connected three-phase converters,” *IEEE Trans. Ind. Appl.*, vol. 37, no. 6, pp. 1817– 1823, Nov./Dec. 2001.
- [10]. P. Jintakosonwitt, H. Fujita, H. Akagi, and S. Ogasawara, “Implementation and performance of cooperative control of shunt active filters for harmonic damping throughout a power distribution system,” *IEEE Trans. Ind. Appl.*, vol. 39, no. 2, pp. 556–564, Mar./Apr. 2003.
- [11]. J. P. Pinto, R. Pregitzer, L. F. C. Monteiro, and J. L. Afonso, “3-phase 4-wire shunt active power filter with renewable energy interface,” presented at the Conf. *IEEE Renewable Energy & Power Quality*, Seville, Spain, 2007.
- [12]. F. Blaabjerg, R. Teodorescu, M. Liserre, and A. V. Timbus, “Over view of control and grid synchronization for distributed power generation systems,” *IEEE Trans. Ind. Electron.*, vol. 53, no. 5, pp. 1398–1409, Oct. 2006.
- [13]. Stein, J., R. Perez, A. Parkins, *Validation of PV Performance Models using Satellite-Based Irradiance Measurements: A Case Study, SOLAR2010, Phoenix, AZ, 2010*
- [14]. Perez, R., J. Schlemmer, D. Renne, S. Cowlin, R. George, B. Bandyopadhyay, *Validation of the SUNY Satellite Model in a Meteosat Environment, Proc., ASES Annual Conference, Buffalo, NY, 2009.*
- [15]. Glasbey, C. A., *Nonlinear autoregressive time series with multivariate Gaussian mixtures as marginal distributions, Applied Statistics* 50: 143-154, 2001.
- [16]. Skartveit, A. and J. A. Olseth, *The probability density and autocorrelation of short-term global and beam irradiance, Solar Energy* 49(6) pp. 477-487, 1992.
- [17]. Tovar, J., F. J. Olmo, L. Alados-Arboledas, *One-minute global Irradiance probability density distributions conditioned to the optical air mass, Solar Energy* 62(6): 387-393, 1998.
- [18]. Tovar, J., F. J. Olmo, F. J. Batlles, L. Alados-Arboledas, *One-minute kb and kd probability density distributions conditioned to the optical air mass, Solar Energy* 65(5), pp. 297-304, 1999

- [19]. Tovar, J., F. J. Olmo, F. J. Battles, L. Alados-Arboledas, Dependence of one- minute global irradiance probability density distributions on hourly irradiation, *Energy* 26, pp. 659-668, 2001
- [20]. Tovar-Pescador, J., Modelling the Statistical Properties of Solar, Radiation and Proposal of a Technique Based on Boltzmann Statistics, in *Modeling Solar Radiation at the Earth's Surface: Recent Advances*, ed. V. Badescu. Berlin, Springer-Verlag, pp. 55-91, 2008
- [21]. Longhetto, A., G. Elisei, C. Giraud, Effect of correlations in time and spatial extent on performance of very large solar conversion systems, *Solar Energy* 43(2), 77- 84, 1989 Data obtained from University of Wyoming College of Engineering web service.